Shaped focal plane detectors for particle concentration and mean size observations

Y. C. Agrawal* and Ole A. Mikkelsen

Sequoia Scientific, Inc., 2700 Richards Road, Bellevue, WA 98005
**yogi.agrawal@sequoiasci.com*

Abstract: We describe a method of designing shaped focal plane detectors for achieving a range of objectives in measurement of particles suspended in a fluid. These detectors can be designed to measure the total concentration in a wide size range (e.g. 200:1) or concentration in a size sub-range (e.g. 63<d<500 μm), and Sauter mean or volume mean diameter. The derivation of these shaped focal plane detectors is rooted in small-angle forward light scattering. The detector shapes are completely general, requiring no assumptions on underlying particle size distribution. We show the theoretical development, numerical simulations and laboratory test results.

©2009 Optical Society of America

OCIS codes: (290.0290) Scattering; (290.5820) Scattering measurements; (040.6070) Solid state detectors; (280.4788) Optical sensors; particles.

References and links

1. Y. C. Agrawal, and H. C. Pottsmith, "Instruments for Particle Size and Settling Velocity Observations in Sediment Transport," Mar. Geol. **168**(1-4), 89–114 (2000).
2. R. J. Davies-Colley, and D. G. Smith, "Turbidity, suspended sediment, and water clarity: a review," J. Am. Water Resour. Assoc. **37**(5), 1085–1101 (2001).
3. T. F. Sutherland, P. M. Lane, C. L. Amos, and J. Downing, "The calibration of optical backscatter sensors for suspended sediment of varying darkness levels," Mar. Geol. **162**(2-4), 587–597 (2000).
4. P. D. Thorne, and D. M. Hanes, "A review of acoustic measurements of small-scale sediment processes," Cont. Shelf Res. **22**(4), 603 (2002).
5. E. D. Hirleman, "Optimal scaling of the inverse Frannhofer diffraction particle sizing problem: the linear system produced by quadrature," Particle Characterization **4**(1-4), 128–133 (1987).
6. Y. C. Agrawal, A. Whitmire, O. A. Mikkelsen, and H. C. Pottsmith, "Light Scattering by Random Shaped Particles and Consequences on Measuring Suspended Sediments by Laser Diffraction," J. Geophys. Res. **113**(C4), C04023 (2008).
7. H. E. Gerber, "Direct measurement of suspended particulate volume concentration and far-infrared extinction coefficient with a laser-diffraction instrument," Appl. Opt. **30**(33), 4824–4830 (1991).
8. E. D. Boss, W. Slade, and P. Hill, "Effect of particulate aggregation in aquatic environments on the beam attenuation and its utility as a proxy for particulate mass," Opt. Express **17**(11), 9408–9420 (2009).
9. H. van de Hulst, Light Scattering by Small Particles. Dover Publications Inc., New York, 470 pp (1981).
10. Y. C. Agrawal, and H. C. Pottsmith, Laser Sensors for Monitoring Sediments: Capabilities and Limitations, a Survey", Federal Interagency Sedimentation Project Meeting, Reno, NV.(2001).
11. D. Topping, S. A. Wright, T. S. Melis, and D. M. Rubin, "High resolution monitoring of suspended sediment concentration and grain size in the Colorado river using laser diffraction instruments and a three-frequency acoustic system, in Proc. of 5th Symposium, Federal Interagency Sedimentation Comm., Reno, NV (2006)

1. Introduction

The concentration, size distribution, and settling velocity distribution of suspended particles are fundamental parameters needed in particle dynamics research and monitoring. Many commercial instruments provide this measurement; a submersible marine version is described by the author [1]. In many situations, less extensive data on particles is sufficient. For example, a simple estimate of concentration C and a mean size d may do. The present paper addresses this need by introducing a new method for obtaining C and d. The described method produces more accurate data than say, turbidity type sensors or single frequency

#117340 - $15.00 USD Received 17 Sep 2009; revised 23 Nov 2009; accepted 1 Dec 2009; published 2 Dec 2009
(C) 2009 OSA

acoustic devices, both of which require recalibration for changing sediment grain size or composition. For example, turbidity type sensors only offer a surrogate for concentration, which is known to suffer from calibration change due to particle size or color, i.e. composition [2,3]. Single wavelength turbidity methods do not yield information on particle size. When size distribution is assumed to be Jungian, attenuation spectra may be employed to estimate the exponent. However, the required assumption of Jungian form is restrictive and not necessarily valid universally. Similarly, acoustic methods suffer from insufficient information to interpret target strength, necessary for derivation of particle size [4]. Shaped focal plane detectors described here can measure particle concentration C with a constant calibration over a wide size range, and with only a very weak sensitivity to composition or color. This is so because the small-angle scattering on which the method is based, is dominated by light diffraction by particles. The diffraction does not depend on particle refractive index, which is what gives particles their color [color arises from dispersion of the real and imaginary parts of the refractive index]. Thus insensitivity to particle composition or color is an advantage where concentration is of interest. We show how the Sauter Mean Diameter (SMD), d_{SMD} which represents the size of spherical particles that would have the same surface to volume ratio as the suspension, is derived. Alternately, a volume mean size is obtainable with yet another shaped focal plane detector. Finally, an extension of these ideas has lead to detector shapes that permit partitioning C into a full size range and a size sub-range. In marine studies on suspended sediment load, such a distinction permits separating fine wash load from local resuspension. We describe the underlying physics, and evaluation of these ideas.

2. Fundamentals of laser diffraction

The present ideas are rooted in small-angle forward light scattering, better known as laser diffraction (LD). To set the stage, a brief introduction is offered. A measurement is made of laser light scattering from an ensemble of particles at n forward angles. This multi-angle scattering data is inverted to construct concentration in n size classes C_n. This is essentially a problem in algebra, solving for n unknowns from equally as many equations. The multi-component concentration vector $\underline{\mathbf{C}}$ containing as its elements the n solutions C_n is called the size distribution. Due to noise in measurements, fewer than n solutions may be obtained in the inversion step. These issues are well understood [5,1].

The attraction of laser diffraction lies in the convenient result that at small angles, light scattering by particles is dominated by diffraction, largely unaffected by particle composition or color. Consequently, any particles can be examined by laser diffraction. For these reasons, LD instruments are widely used in science and industry.

The diffraction patterns of illuminated ensemble of particles in a beam, Fig. 1, add incoherently (i.e. the intensities add together). Consequently, the overall diffraction pattern of the ensemble is the sum of the patterns for each size of particle, weighted by its concentration.

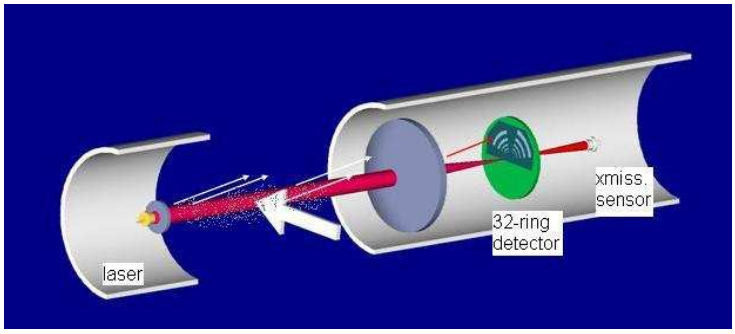

Fig. 1. Schematic of a laser diffraction set up, showing *left to right,* a collimated beam, a receiving lens, and a set of ring detectors in the focal plane of a receiving lens.

#117340 - $15.00 USD Received 17 Sep 2009; revised 23 Nov 2009; accepted 1 Dec 2009; published 2 Dec 2009
(C) 2009 OSA

The weighted sum can be expressed in terms of a matrix product as:

$$\underline{E} = \underline{\underline{K}}\,\underline{C} \tag{1}$$

where $\underline{\mathbf{E}}$ is a column vector, elements of which represent scattered light energy sensed at multiple forward angles, $\underline{\underline{\mathbf{K}}}$ is a kernel matrix, and $\underline{\mathbf{C}}$ is an n-element column vector representing the size distribution. Inversion of this equation produces the desired solution for the size distribution $\underline{\mathbf{C}}$. In this paper, we will use $n = 32$, which is applicable to the instrument described by Agrawal and Pottsmith [1], and used in experiments here.

Before leaving this discussion, we note that even though this description of $\underline{\underline{\mathbf{K}}}$ is based on diffraction, in modern times the kernel matrix has typically been computed using Mie theory which applies for homogeneous spheres, so that light refraction through particles is also included in the total scattering. Recently, new empirical data have been acquired so that a more suitable matrix for random shaped particles replaces Mie theory [6] With the initial application of this work being in marine science, this paper employs the kernel matrix for randomly shaped terrigenous particles (crushed rock) which are available as ISO-12103-1 standard particles from Powder Technology Inc., Burnsville, Minnesota, USA.

3. Definitions

We shall use the term concentration hereafter generally to mean volume concentration of particles, e.g. *µl/l.* Alternate uses include area concentration, number concentration etc. We also define two diameters which appear later in the text. Variables with subscripts v and A will refer, respectively, to volume and area.

3.1 Sauter mean diameter (SMD)

The SMD is relevant to studies where particle volume and area concentration are both important. This is true in pollutant transport where attachment of pollutants to particle surfaces is important. The term is commonly used in the combustion of fuel droplets. Denoting the total scalar volume concentration as C_v and area concentration as C_A, the SMD is defined as:

$$d_{SMD} = 1.5\mathrm{C_v} / \mathrm{C_A} \tag{2}$$

3.2 Volume mean diameter (VMD)

Because the volume distribution measured with LD devices is commonly presented in log-spaced size classes, it is important to be careful with the definition of the VMD. Since log-normal and other logarithmic form distributions are not readily intuitive, we explain this briefly.

Let the logarithmically spaced sizes d_i (diameters) of a laser diffraction set up be represented by:

$$d_i = d_1 \rho^{i-1} \tag{3}$$

where i represents the size class, ranging from 1 to n, and ρ is ratio of size in bin i to i-1. If one defines an integer u_i as

$$u_i = \log(d_i / d_1) / \log(\rho) \tag{4}$$

then, u_i takes values 1 to $n + 1$ and represents lower size in a size bin. The center of each size bin is $\sqrt{(d_{i+1} \bullet d_i)}$. Hereafter, we refer to this size as the bin size.

Let the size distribution be described by the form $p(u)$ then the mean size bin $\boldsymbol{u}$ is, by definition:

#117340 - $15.00 USD Received 17 Sep 2009; revised 23 Nov 2009; accepted 1 Dec 2009; published 2 Dec 2009
(C) 2009 OSA

$$\boldsymbol{u} = \sum i u_i \, p(u_i) / \sum p(u_i) \tag{5}$$

where $\boldsymbol{u}$ represents the bin number containing the center of moment of the size distribution, *i.e.* the mean logarithmic diameter. $\boldsymbol{u}$ need not be an integer.

From Eqs. (4) and (5), the VMD is:

$$VMD = d_1 \rho^{\boldsymbol{u}-1} \tag{6}$$

where d_1 is the *inner* diameter of the first size bin. In other words, the bin number of the mean size appears in the exponent of the parameter ρ. Of course, $\boldsymbol{u}$ may take any value within the range covered by the size bins.

In the formulation later for getting the VMD from a shaped detector, we shall aim to get the mean value, $\boldsymbol{u}$.

4. Origin of shaped focal plane detectors

We next derive a variety of focal plane detectors. All shapes result from asking this question: is there a set of weight factors (elements of a vector) which can be used to construct a weighted sum of light seen by the ring detectors of Fig. 1 and which results in the desired measurement.

4.1 A Detector for sensing total volume concentration

Here, we search for weight factors, i.e. row vector $\underline{\mathbf{T}}_{\mathbf{v}}$, such that the scalar product:

$$\underline{\mathbf{T}}_{\mathbf{v}}\mathbf{E} = \gamma_v C_v \tag{7}$$

where γ_v is a calibration factor. In other words, we are seeking 32 weight factors (elements of the row vector $\underline{\mathrm{T}}_{\mathrm{v}}$) such that the weighted sum of Eq. (7), $\sum i \mathrm{T}_{\mathrm{v}i}\mathrm{E}_i$, represents the total concentration C_{v}, where C_{v} itself is the sum of all components of the size distribution - the vector $\underline{\mathbf{C}}_{\mathbf{v}}$. The weighted sum C_{v} is next represented as a scalar product of a unit vector $\underline{\mathrm{U}}$ with the size distribution vector $\underline{\mathbf{C}}_{\mathbf{v}}$:

$$\begin{aligned} \underline{\mathbf{U}}\underline{\mathbf{C}}_{\mathbf{v}} &= \sum i \underline{\mathbf{C}}_{\mathbf{v}i} \\ &= \mathbf{C}_{\mathrm{v}} \end{aligned} \tag{8}$$

so that substituting from Eq. (1) for $\underline{\mathbf{E}}$ in Eq. (7) and using Eq. (8), we have:

$$\underline{\mathbf{T}}_{\mathrm{v}}(\underline{\underline{\mathbf{K}}}_{\mathrm{v}}\underline{\mathbf{C}}_{\mathrm{v}}) = \gamma_{\mathrm{v}}\underline{\mathbf{U}}\underline{\mathbf{C}}_{\mathrm{v}} \tag{9}$$

which yields the solution for the weight factors $\underline{\mathbf{T}}_{\mathrm{v}}$ as the matrix product:

$$\underline{\mathbf{T}}_{\mathrm{v}} = \gamma_{\mathrm{v}}\underline{\mathbf{U}}\underline{\underline{\mathbf{K}}}_{\mathrm{v}}^{-1} \tag{10}$$

Note now that we have used the subscript v for $\underline{\underline{\mathbf{K}}}$ beginning in Eq. (9), to explicitly mean a kernel matrix, each row of which is the scattering across ring detectors for unit *volume* concentration of a particular size class. Equation (10) forms the essence of the current idea. Again, γ_{v} being simply a system constant absorbing optical and electronic factors, can be set to unity. It can be dealt with in system calibration. If the solution to Eq. (10) exists, then a simple weighted sum according to Eq. (7) yields the total concentration. The solution in the form of Eq. (10) was first noted in the context of measuring the liquid water content of clouds [7].

#117340 - $15.00 USD Received 17 Sep 2009; revised 23 Nov 2009; accepted 1 Dec 2009; published 2 Dec 2009
(C) 2009 OSA

It is notable that the derivation of the vector $\underline{\mathbf{T}}_v$ is independent of the size distribution $\underline{\mathbf{C}}_\mathbf{v}$. In other words, the weight factors are generally applicable for any size distribution, without restriction to the shape of $\underline{\mathbf{C}}_\mathbf{v}$.

The weight factors depend on the kernel matrix only, Eq. (10). Thus, the assumptions built into the construction of the kernel matrix apply. For example, the size-range within which the size-classes are defined is identical to the size-range of the corresponding LD instrument, *i.e.* the maximum and minimum particle diameters are related to the minimum and maximum scattering angles θ covered by the ring detectors, respectively, i.e.

$$a_{min} = 2 / k\theta_{max}; \tag{11}$$

$$a_{max} = 2 / k\theta_{min}; \tag{12}$$

and

$$\theta_{min,max} = \arctan(r_{min,max} / f) \tag{13}$$

where $k = 2\pi/\lambda_o$; λ_o is optical wavelength, and $r_{min,\ max}$ are the inner radius of the smallest ring detector, and the outer radius of the largest ring detector, respectively. The receiving lens focal length is f.

It is notable that the solutions of Eq. (10) are applicable only for volume concentration. A growing body of literature in marine science notes that the larger particles tend to be aggregates of fractal dimensions approaching 2 [8]. That is, aggregates conserve area of the constituent particles, and their mass density varies as $1/d$. Thus, while the methods here are applicable to estimating volume concentration generally, conversion to mass concentration should be done with care when working in the marine environment.

4.2 A shaped detector for sensing volume concentration in a size sub-range

Equation (7) hints at the possibility of finding a different set of weight factors to sum the concentration in a sub-range of the size distribution. For example, it is possible to seek weight factors $\underline{\mathbf{T}}$ such that one obtains the concentration that excludes the lower m size classes. If $\underline{\mathbf{U}}$ is replaced by a vector $\underline{\mathbf{U}}_2$ that contains zeros in its first m of 32 elements, and ones elsewhere, one would construct a weight factor $\underline{\mathbf{T}}$ that, when used with $\underline{\mathbf{E}}$ to construct a weighted sum, delivers a concentration in the size classes $m + 1$ to 32. In this way, a coarse fraction sensor can be designed. One can take this idea further in principle, and seek a set of weight factors that produce concentration in a single size bin, effectively looking for particles only of a particular size. However, this is not practical due to the properties of the kernel matrix, specifically its eigenvectors and condition number. The subject is more complex and mathematical than the scope of the present paper. Suffice it to say that within the limitations of the properties of the kernel matrix, concentration in a specific range of sizes can be extracted by the method of weighted sum in Eq. (10). The vector $\underline{\mathbf{U}}_2$ permits the construction of a coarse particle sensor:

$$\begin{aligned} \underline{\mathbf{T}}_{v2} &= \gamma_v \underline{\mathbf{U}}_2 \underline{\underline{\mathbf{K}}}_v^{-1}, \quad \text{where} \\ \underline{\mathbf{U}}_2 &= [0\,0\,0\ m \text{ times} \ldots 1\,1\,1 \ldots 32 - m \text{ times}.]; \end{aligned} \tag{14}$$

4.3 A detector for sensing area concentration

In a manner exactly parallel to the derivation of Eq. (10), one can derive weight factors that, when used to form the scalar sum $\underline{\mathbf{T}}_\mathbf{A} \bullet \underline{\mathbf{E}}$, yield the particle area concentration (cm^2/liter). The solution then is, following Eq. (10):

#117340 - $15.00 USD Received 17 Sep 2009; revised 23 Nov 2009; accepted 1 Dec 2009; published 2 Dec 2009
(C) 2009 OSA

$$\underline{\mathbf{T}}_{\mathbf{A}} = \gamma_A \underline{\underline{\mathbf{K}}}_{\mathbf{A}}^{-1} \underline{\mathbf{U}} \tag{15}$$

where the corresponding kernel matrix $\underline{\underline{\mathbf{K}}}_{\mathbf{A}}$ is based on particle area concentration, *i.e.,* each row of the kernel matrix represents light scattering per unit area concentration of particles. Although such weight factors are interesting, one need not use this method. The optical obscuration obtains an excellent estimate of the area concentration but for the case of very fine particles ($a \sim \lambda_o$). Only then, the above weight factors provide an improvement over optical obscuration. This is due to the fact that scattering efficiencies depart from being 2 for such small particles. For further details, see van de Hulst [9].

4.4 A detector for sensing volume mean diameter

In many applications the SMD is not relevant; instead the volume mean diameter is of interest. In this case, we are seeking the ratio of the first moment of the size distribution $\underline{\mathbf{C}}_{\mathbf{v}}$ divided by the total concentration C_v. Thus, we seek a set of weight functions $\underline{\mathbf{T}}_{\mathbf{D}}$ such that, in a manner similar to Eq. (7):

$$\underline{\mathbf{T}}_{\mathbf{D}} \underline{\mathbf{E}} = \gamma \underline{\mathbf{R}} \underline{\mathbf{C}}_v \tag{16}$$

where

$$\underline{\mathbf{R}} = [1:32] \tag{17}$$

is a ramp function, representing size bin numbers. The right hand side of Eq. (16) represents the first moment of $\underline{\mathbf{C}}_{\mathbf{v}}$, so that the mean size is the size in bin R_m:

$$R_m = \underline{\mathbf{R}} \underline{\mathbf{C}}_{\mathbf{v}} / \underline{\mathbf{U}} \underline{\mathbf{C}}_{\mathbf{v}} \tag{18}$$

Solving Eq. (16) in a manner similar to the method of Eq. (10) produces weight factors that are extremely sharply peaked for the smallest ring detectors. Such highly peaked functions are not desirable since small errors in the light falling on the inner detector rings can produce large errors in the resulting value of R_m. To find less strongly peaked weight factors, we solve for a linearly related variable $\underline{\mathbf{X}}$, defined as:

$$\underline{\mathbf{X}} = 6.6 - 0.2\underline{\mathbf{R}} \tag{19}$$

Or,

$$\underline{\mathbf{X}} = [6.4 : -0.2 : 0.2] \tag{20}$$

The inversion parallels Eq. (10):

$$\underline{\mathbf{T}}_{\mathbf{D}} = \underline{\underline{\mathbf{K}}}_{\mathbf{v}}^{-1} \underline{\mathbf{X}} \tag{21}$$

from which,

$$X_m = \underline{\mathbf{T}}_{\mathbf{D}} \underline{\mathbf{E}} / \underline{\mathbf{T}}_{\mathbf{v}} \underline{\mathbf{E}} \tag{22}$$

The denominator is the total volume concentration, which is yielded by the volume sensing detector. From Eq. (19) the bin number for the mean diameter is:

$$R_m = 5(6.6 - X_m) \tag{23}$$

from which:

$$d_m = d_1 \rho^{[R_m - 1]} \tag{24}$$

#117340 - $15.00 USD Received 17 Sep 2009; revised 23 Nov 2009; accepted 1 Dec 2009; published 2 Dec 2009
(C) 2009 OSA

By performing the transformation of Eq. (19), the weight factor for the inner detector rings are reduced, and the dynamic range of $\underline{\mathbf{T}}_{\mathbf{D}}$ is also reduced. It makes $\underline{\mathbf{T}}_{\mathbf{D}}$ even less peaked than $\underline{\mathbf{T}}_{\mathbf{v}}$ as we show next.

5. Results

5.1 Solutions for weight factors $\underline{T}$

We show 3 cases: (*i*) direct total volume concentration estimation; (*ii*) volume estimation in a size sub-range; and (*iii*) mean size estimation. To solve for the weight factors according to Eqs. (10), (14) and (21), we have employed the Philips-Twomey method, which permits controlled smoothing of the result. Smoothing is desired to keep the resulting shapes from becoming too complex to fabricate, which would defeat some of the purpose of the focal plane detector design. However, smoothing comes at some expense to the accuracy of Eq. (7). An optimal solution is selected in all cases based on desired smoothing and fidelity of achieving a perfect result.

Figure 2 shows the weight factors to find the total volume concentration ($\underline{\mathbf{T}}_{\mathbf{v}}$) over the size-range 2.5 to 500 μm; concentration in a size sub-range d >63 μm ($\underline{\mathbf{T}}_{\mathbf{v2}}$), and to find the moment of the size distribution for estimating the volume mean size. Note that of these, the dynamic range of variation of $\underline{\mathbf{T}}_{\mathbf{v2}}$ is the smallest. This is why the transformation of Eq. (18) was employed. In contrast, the other two volume estimators $\underline{\mathbf{T}}_{\mathbf{v}}$ and $\underline{\mathbf{T}}_{\mathbf{v2}}$ vary over the largest dynamic range, both exhibiting the strongest weighting for the inner ring detectors and near-zero (but not zero!) weighting for outer ring detectors.

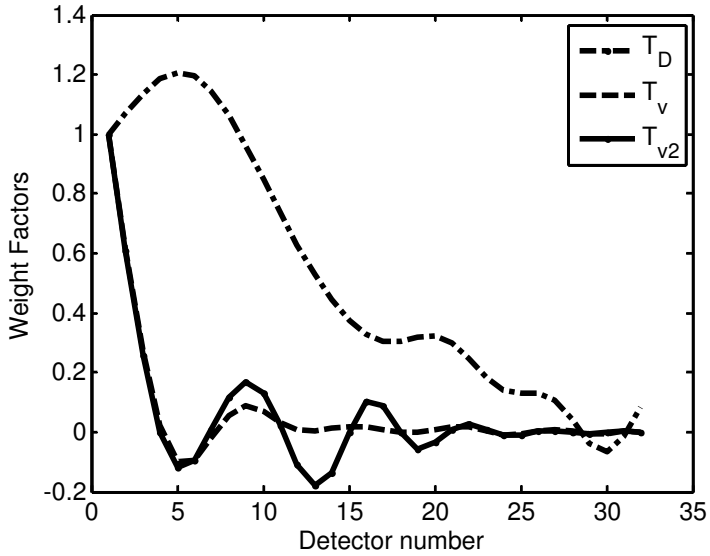

Fig. 2. Normalized weight factors for $\underline{\mathbf{T}}_{\mathbf{D}}$, $\underline{\mathbf{T}}_{\mathbf{v}}$, and $\underline{\mathbf{T}}_{\mathbf{v2}}$. These magnitudes scale with the magnitude of corresponding matrix $\underline{\mathbf{K}}$.

5.2 Shaped detectors

The implementation of physical systems to estimate concentrations and mean sizes following the preceding ideas can be done in many ways. The first and most obvious is to measure the data vector $\underline{\mathbf{E}}$ and perform the weighted sum digitally in post-processing. This was employed for testing these ideas in the laboratory. Second, it is possible to sum of the output of the 32 pre-amplifier stages in a summing amplifier to produce the weighted sum. The third method

#117340 - $15.00 USD Received 17 Sep 2009; revised 23 Nov 2009; accepted 1 Dec 2009; published 2 Dec 2009
(C) 2009 OSA

produces the greatest simplification – to form shaped detectors. The attraction of shaped detectors lies in the simplicity of downstream electronics – a simple amplifier is all that is required before digitization of the measurement.

The 'comet' shape arises as follows. Let us begin with the multi-ring detector shown in Fig. 1. Now, adjust the azimuthal width of each of the ring detectors in proportion to its weight factor. As the weight factors decrease rapidly away from center, the azimuthal width will decrease. The larger radius detectors become thinner in azimuth. One then (conceptually) joins these azimuth-adjusted ring detectors to implement the addition. This produces a comet-like detector, with a head and 'blobs' that have a positive and negative response. This is shown in Fig. 3. A single comet detector is sufficient to estimate volume concentration C_v, and in combination with extinction of the beam for estimating particle area concentration, this produces the SMD. To get the VMD, one needs two comets to implement the scalar products $\underline{\mathbf{T}}_{\mathbf{D}}\underline{\mathbf{E}}$ and $\underline{\mathbf{T}}_{\mathbf{v}}\underline{\mathbf{E}}$. The comets can be placed in opposing halves of the detector plane. In this case, the beam attenuation is not necessary.

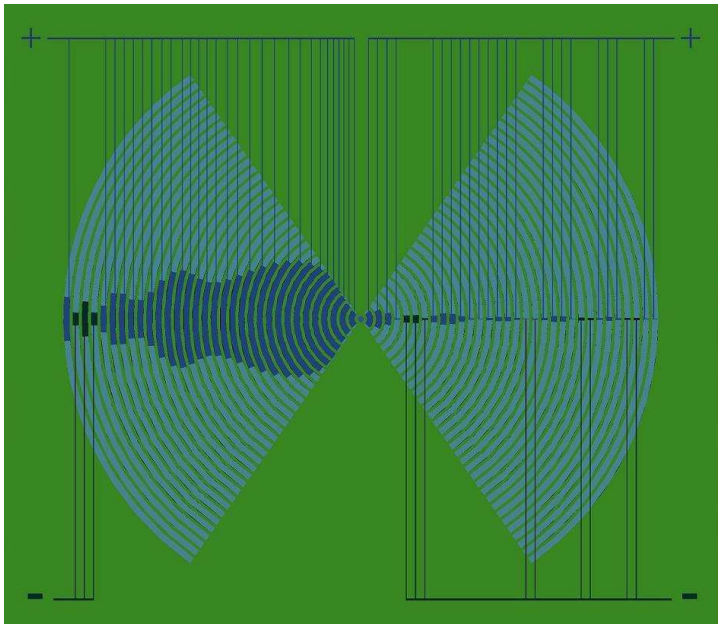

Fig. 3. The formation of the comet shape by modulating azimuth or arc-width of each detector in proportion to the weight factors. The inner-most rings cover a 120-degree arc-width. The detectors with positive weights are connected together, and likewise, negatives are also connected together. The darker parts are the active areas. This is the conceptual view. In reality, all positive elements would be contiguous, and negative elements would be similarly contiguous, thus forming comet-shaped detectors. The thin comet on right measures volume concentration, while the fat one on left finds the constant *X*.

5.3 Numerical simulations and laboratory tests

For simulations, we use the parameters of the LISST-100 instrument manufactured by Sequoia Scientific, Inc. The minimum and maximum sizes are 2.5 to 500 microns, respectively, and $\rho = 1.1809$.

To numerically test the fidelity of the weight factors for concentration in the full and sub-ranges, [refer Eq. (10)] we plot the ratios $\underline{\underline{\mathbf{K}}}_{\mathbf{v}}\underline{\mathbf{T}}_{\mathbf{v}} / \underline{\mathbf{U}}$ and $\underline{\underline{\mathbf{K}}}_{\mathbf{v}}\underline{\mathbf{T}}_{\mathbf{v2}} / \underline{\mathbf{U}}$. These should mirror $\underline{\mathbf{U}}$ and $\underline{\mathbf{U}}_2$ respectively, for ideal weight factors. We call these ratios the fidelity factors, shown in Fig. 4. For this test, the kernel matrix $\underline{\underline{\mathbf{K}}}_{\mathrm{v}}$ that was employed was for random shaped particles [6]. It is seen that the concentration over the full size range C is faithfully produced for the

#117340 - $15.00 USD Received 17 Sep 2009; revised 23 Nov 2009; accepted 1 Dec 2009; published 2 Dec 2009
(C) 2009 OSA

entire size range within an error of no more than ~5%. This is to be contrasted with a *factor* of 200 error that would occur over the 200:1 size range with simple turbidity type sensors. The fidelity of the sub-range sensor shows a less than ideal response. Although fines are ignored, as desired, the edge between fines and coarse particles is not sharp. This is the limitation resulting from the properties of kernel matrix and its eigen-vectors. Thus, the sub-range estimator should be considered approximate. To test for the validity of estimating the volume mean diameter, we treat each row of the kernel matrix $\underline{\underline{\mathbf{K}}}_v$ as data vector $\underline{\mathbf{E}}$. Substituting in Eqs. (22-23), first X_m, then R_m is computed, and d_m is computed from Eq. (24). The fidelity test parameter then is the ratio $d_m / (d_1 \rho^i)$ for row i, which represents size class i.

Next, we report results of laboratory tests to evaluate how well the above ideas on concentration estimators work in contrast to area-based optical sensors, Fig. 5. Two sets of data are displayed. The near-horizontal set (*) is the fidelity of total concentration measurement, *i.e.* ratio of estimated to true concentrations, for random shaped natural particles. These particles spanned the size range from 3.5 microns to 450 microns. All but the 3 points at the smallest diameters are for narrow size distributions, ¼-ϕ wide. The first 3 points are for dusts with relatively wider size distribution, obtained from Particle Technology Inc. These were in size fractions 2-6, 4-8, and 6-11 microns, at the 10 and 90% points of the cumulative distributions. Also shown is the fidelity of concentration estimated from an area-based optical sensor, *i.e.* from the transmissometer function of the LISST-25 (o). It shows a 2-order magnitude variability in output. Clearly, the $\underline{\mathbf{T}}_v$ weight factors and the resulting comet detector provide a high-fidelity measurement of sediment concentration. The area-based sensor responds to sediment concentration with a 1/*d* size dependence, as is well known.

In all 3 cases, only the largest size class performs poorly, with a ~20% error for all 3 fidelity parameters. Very similar results are obtained for area distributions [2].

The fidelity of mean diameter estimation is shown in Fig. 6. Data are from the same set of particles as in Fig. 5. The particle mean diameter estimate is within about 20% throughout from about 3 to 500 microns. Some of the scatter in the data may be attributable to imperfect mixing.

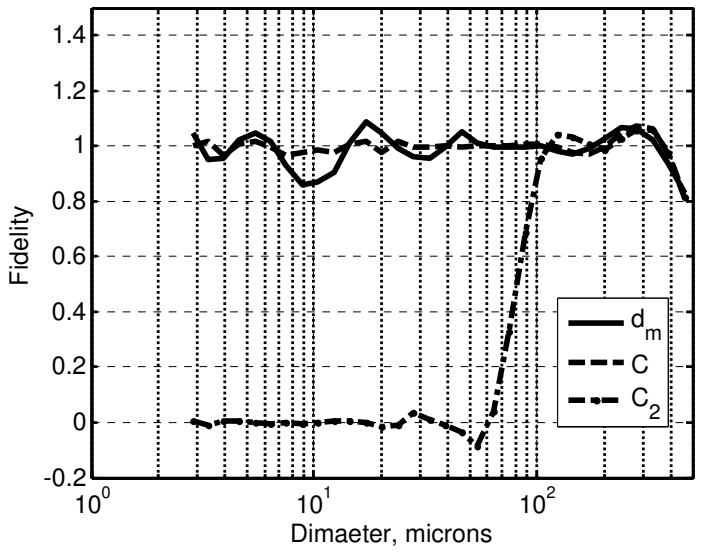

Fig. 4. Numerical simulations: Fidelity testing of weight functions for estimating mean diameter, total, and sub-range concentrations. (The ordinate is fidelity).

#117340 - $15.00 USD Received 17 Sep 2009; revised 23 Nov 2009; accepted 1 Dec 2009; published 2 Dec 2009
(C) 2009 OSA

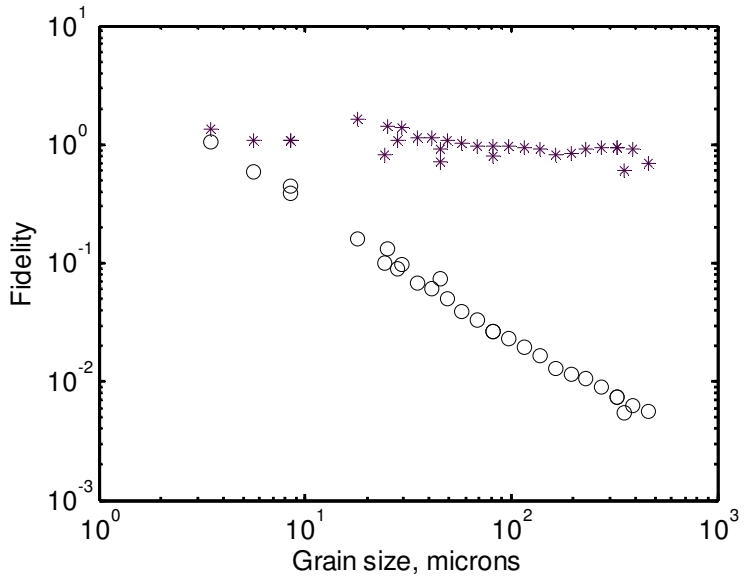

Fig. 5. Fidelity of measurement of concentration of random shaped natural grains. The weighted sum (*) shows a near constant value. In contrast, an optical transmission-based estimate (o) shows essentially 1/*d* dependence, producing a 2-order of magnitude variation in calibration.

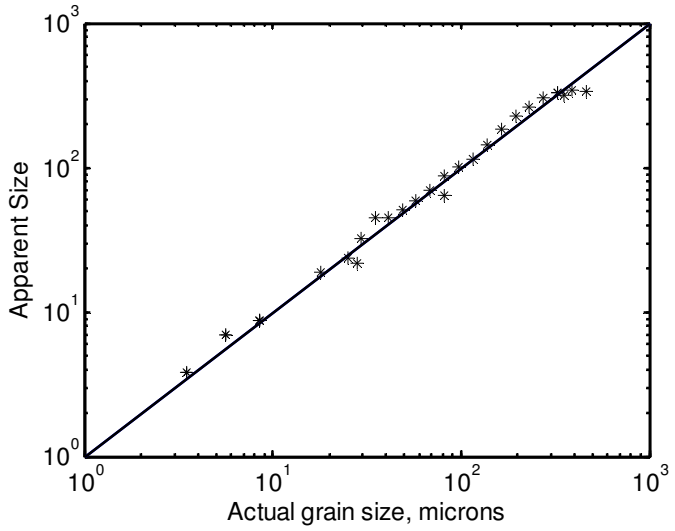

Fig. 6. Fidelity of estimation of mean diameter (*). The straight line is 1:1.

The final laboratory test is to evaluate the weight factors $\underline{\mathbf{T}}_{\mathbf{v2}}$ which produces a concentration of coarse particles only. Again, the same data used for Figs. 5 and 6 are employed and the scalar sum according to Eq. (12) was obtained for each particle size. The results are shown in Fig. 7. The fine particles are essentially 'invisible' to this sensor, and the response rises to good fidelity over the size range 60-90 microns. The response is similar to the prediction shown in Fig. 4.

#117340 - $15.00 USD Received 17 Sep 2009; revised 23 Nov 2009; accepted 1 Dec 2009; published 2 Dec 2009
(C) 2009 OSA

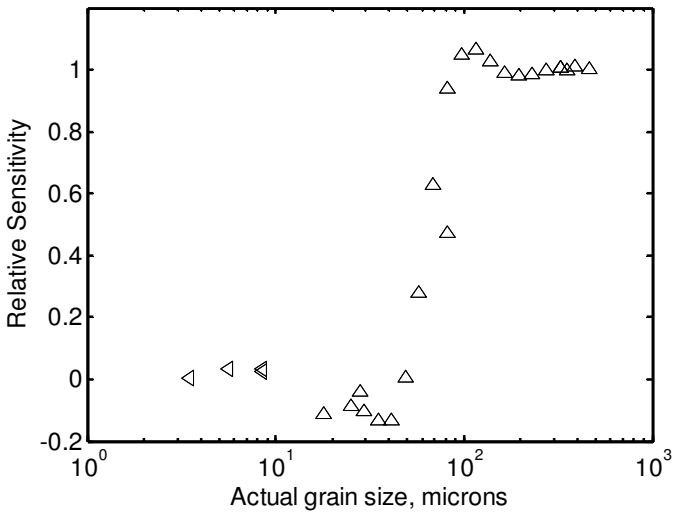

Fig. 7. Effectiveness of the coarse-particle sensor weight factors $\underline{T}_{v2}$. This relative sensitivity to particles of different sizes closely mirrors the theoretical response of Fig. 4.

It is reasonable to ask how these comet-type sensors would see particles that are outside the range of diameters. We have addressed this question elsewhere in context of the LISST-100 [10]. The same applies to concentration sensors also. Briefly, particles smaller than the measurement range 'leak' into the smallest size classes within the measurement range, with leakage decreasing to zero for particles smaller than a factor of 10 than the smallest particles within measurement range. Similarly, particles larger than the largest in measurement range leak in to the largest size bins within the measurement. The leakage of larger sizes drops off sharply, reaching small values for particles larger by just a factor 2.

6. LISST-25X: A marine instrument

A commercial instrument LISST-25X has been marketed by the author's company under US patent 6466318. Although the principle of the device was described in the Patent via Eq. (10), the remaining analysis presented here has not previously been offered. Simulation and laboratory tests have also not been reported until this paper. The instrument incorporates a collimated 670nm laser, and a 120 mm focal length collecting lens similar to the LISST-100 type-C instrument, i.e. nominal particle size range 2.5 to 500 microns. A ring detector is used and the weighted sums are directly computed in the firmware of the instrument at present. Each data record stores the following parameters: total concentration, concentration in the coarse sub-range, the SMD of the total and coarse sub-range, and optical transmission, time and depth. A TFX-11 micro-computer (Onset Computers, Massachusetts) is employed for analog to digital conversion of the signals, for data scheduling, and data storage. The instrument is equipped with sufficient memory to store nearly 500K samples. The instrument operates on 4 9-V alkaline batteries, included in the housing. The instrument measures 10cm dia. x 60 cm long, and weighs 4.5 kg in air (1.5 kg when submerged). Depth capability is 300m, and the depth measurement has a resolution of 7.5cm. Field deployment is done with the instrument horizontal, so that particles do not settle on the windows. Field data were presented by Topping et al. [11] showing excellent agreement between the LISST-25X measurements and physical samples as well as acoustic estimates. The acoustic estimates were derived with a calibration based on a mix of physical samples and assumption of spatial homogeneity of sediment distribution in the vigorous, turbulence-stirred river. Without the latter assumption, concentration cannot be derived from single frequency acoustics.

#117340 - $15.00 USD Received 17 Sep 2009; revised 23 Nov 2009; accepted 1 Dec 2009; published 2 Dec 2009
(C) 2009 OSA

7. Summary

We have presented general solutions to the construction of weight functions which when used to construct weighted sums with multi-angle scattering produce estimates of concentration or mean size of suspended particles. The method does not constrain the shape of the size distribution, but instead, restricts the size range for which the solutions apply. The size range is broad, 200:1. The weight factors can be used to visualize various shaped focal plane detectors to obtain a desired result: total concentration, concentration in a sub-range of sizes, and mean sizes. The method applies to spherical particles or any other shaped particles whose scattering particles are known and can be modeled in the matrix **K**. Laboratory tests confirm the predictions. Errors in obtaining perfect response for all size particles are orders of magnitude smaller in contrast to other methods such as optical obscuration.

Acknowledgements

This work was done while YCA was partially supported from the Office of Naval Research, Contract No N00014-04-C-0433 and OAM was supported by Sequoia internal research and development funds. H.C. Pottsmith and colleagues from Sequoia contributed to data collection.

#117340 - $15.00 USD Received 17 Sep 2009; revised 23 Nov 2009; accepted 1 Dec 2009; published 2 Dec 2009
(C) 2009 OSA